Polarization and Anisotropy of the Microwave Sky

D. Coulson,[1,2] R. G. Crittenden,[1] and N. G. Turok[1]

[1]*Joseph Henry Laboratory, Princeton University, Princeton, New Jersey 08544*

[2]*The Blackett Laboratory, Imperial College, London SW7 2BZ, United Kingdom*

(Received 15 June 1994)

We study the polarization-polarization and polarization-temperature correlations in standard adiabatic scenarios for structure formation. Temperature anisotropies due to gravitational potential wells and oscillations in the photon-baryon-electron fluid on the surface of last scattering are each associated with a correlated polarization pattern. While the "correlated part" of the polarization has an rms of only a third of the total signal, it may still be measurable by mapping a large area on the sky. We calculate the expected signal to noise ratio for various measures of the polarization in a hypothetical mapping experiment such as those now being planned.

PACS numbers: 98.70.Vc, 98.80.Cq, 98.80.Es

Since detection by the Cosmic Background Explorer satellite of anisotropies in the cosmic background radiation (CBR) [1], attention has focused on obtaining higher resolution measurements, and ultimately maps of the temperature anisotropies on the sky. The angular correlations and statistics of the anisotropy pattern will yield valuable clues as to the formation of large scale structure in the Universe—whether the perturbations were adiabatic or isocurvature, Gaussian or non-Gaussian, whether there was a significant gravity wave component, or if cosmic defects were involved. However, there is substantial degeneracy among the predictions of different theories [2–4], and it is worth asking whether any additional information that might further discriminate between theories could be extracted from the microwave sky.

The idea that the polarization of the microwave sky might provide such additional information is not new (see, e.g., [5–8]), and some experimental limits have already been set [9–11]. The expected level of linear polarization is low (typically 5% of the anisotropy), but with experiments currently being planned to map the sky temperature to an accuracy of 3 μK per pixel, one is clearly close to the level required for a measurement.

In this Letter, we extend previous work [7] to consider the temperature-polarization cross correlation function $\langle QT \rangle$. (Throughout, T refers to the temperature anisotropy and Q and U are the Stokes parameters which describe the polarization [12].) We discuss the advantages this has as an observable when the detector noise per pixel is larger than the signal and show that it may be measurable in experiments with large sky coverage such as those currently being proposed.

Why should the polarization of the sky be correlated with the temperature anisotropy? The linear polarization produced by Thomson scattering is proportional to the quadrupole moment of the incident photon phase space density. At redshifts >1300, the photons, baryons, and electrons constitute a tightly coupled fluid, in which the quadrupole is vanishingly small. But as photons decouple, fluctuations in the temperature, fluid velocity, and gravitational potential about a scattering electron lead to a quadrupole in the radiation incident upon it. The dominant effect results from a converging or diverging velocity field which produces, through the Doppler effect, a quadrupole of order $\tau \nabla v_r \sim -\tau \dot{\delta}_r$, with τ the mean free time for Thomson scattering, δ_r and v_r the density and velocity perturbations.

Consider a potential well on the "surface of last scattering," appearing to us as a cold spot on the microwave sky. As it enters the horizon, gravitational forces cause the surrounding matter to fall into the well [Fig. 1(A)]. The converging velocity field induces a local radiation quadrupole at points on the edge of the well, causing an excess of scattered light polarized radially about the cold spot [Fig. 1(B)]. Similarly, a potential hill (a temperature hot spot) produces a diverging velocity field and thus a *tangential* polarization pattern. After a radiation perturbation enters the horizon, it oscillates acoustically, with the temperature and velocity field oscillating out of phase. At a fixed time (decoupling), the phase of the oscillations varies as a function of wavelength, so the relation between temperature and polarization alternates sign as one moves to smaller scales (Fig. 2).

The gravitational potential also creates a quadrupole. A point on the edge of a potential well sees less energetic photons coming from the well, which leads to a *radially* polarized pattern about temperature cold spots. This

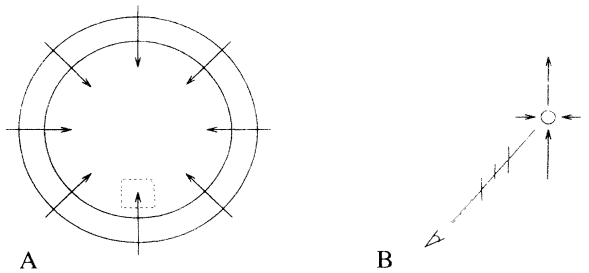

FIG. 1. Converging velocity flows cause a radial polarization pattern. The velocity field in the box in (A) is enlarged in (B) to show the induced polarization.

 0031-9007/94/73(18)/2390(4)$06.00

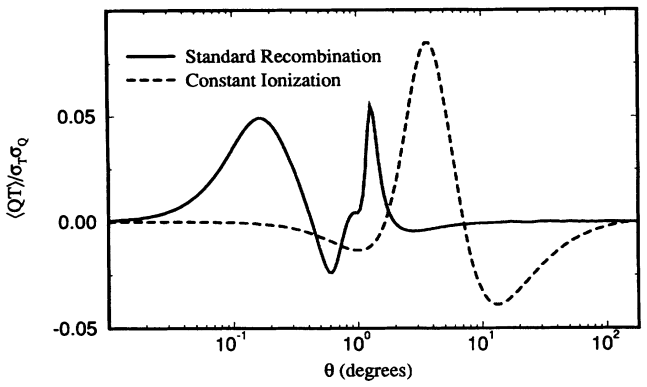

FIG. 2. QT correlation function in units of $\sigma_T\sigma_Q$, where σ_T^2 is the temperature anisotropy variance and σ_Q^2 is the total polarization variance. Shown are results for a universe with standard recombination and a fully ionized universe with no recombination.

effect has the same sign as the convergent velocity field discussed above, and presumably both contribute to the negative tail in $\langle QT\rangle$ on large angular scales. Primordial gravity waves also lead to anisotropy and polarization in the CBR [13], which may have a distinct $\langle QT\rangle$ signature on large angular scales. We shall investigate this in future work.

To calculate the two-point correlation functions, we evolve the photon distribution function $\mathbf{f}(\mathbf{x},\mathbf{p},t)$ [14]. We assume the initial perturbations are adiabatic, pure growing modes. Here we study an $\Omega = 1$, $\Omega_B = 0.05$, and $h = 0.5$ cold-dark-matter dominated universe with standard thermal history and a universe with no recombination (an extreme example of a reionized universe).

The initially Planckian, unpolarized photon distribution function is evolved forward using the general relativistic Boltzmann equation for radiative transfer with a Thomson scattering source term. For simplicity we consider only scalar perturbations. In this case one needs to evolve only two transfer equations, for the components of $\mathbf{f}$ corresponding to Stokes' parameters I and Q [15]. These equations are written in terms of brightness functions, $\Delta^i \equiv 4\delta f_i/(T_0\,\partial\bar{f}/\partial T_0)$, where T_0 is the mean CBR temperature, $\bar{f}$ is the unperturbed Planck distribution, δf_i is its first order perturbation, and $i = T, P$.

The computational scheme is that of Bond and Efstathiou [7,14]. We expand the cosmological perturbations in plane waves and the brightness functions in spherical harmonics, converting the transfer equations to a hierarchy of ordinary differential equations.

Once evolved to the present epoch, the Legendre expansion coefficients Δ_l^i $(i = T, P)$ are used to construct the temperature and polarization correlation functions

$$\langle T(\hat{\mathbf{q}})T(\mathbf{e_z})\rangle = \sum_l (2l+1)C_l^T P_l(\cos\theta), \quad (1)$$

$$\langle Q(\hat{\mathbf{q}})T(\mathbf{e_z})\rangle = \cos 2\phi \sum_{l\geq 2} (2l+1)C_l^{TP} P_l^2(\cos\theta), \quad (2)$$

$$\langle U(\hat{\mathbf{q}})T(\mathbf{e_z})\rangle = \sin 2\phi \sum_{l\geq 2} (2l+1)C_l^{TP} P_l^2(\cos\theta), \quad (3)$$

$$\langle Q(\hat{\mathbf{q}})U(\mathbf{e_z})\rangle = \sin 4\phi \sum_{l\geq 4} (2l+1)C_l^{PP} P_l^4(\cos\theta), \quad (4)$$

$$\langle Q(\hat{\mathbf{q}})Q(\mathbf{e_z})\rangle = \sum_l (2l+1)\,C_l^P P_l(\cos\theta) + \cos 4\phi \sum_{l\geq 4} (2l+1)C_l^{PP} P_l^4(\cos\theta), \quad (5)$$

where (θ, ϕ) are the usual spherical polar angles, $\hat{\mathbf{q}} = (\sin\theta\cos\phi, \sin\theta\sin\phi, \cos\theta)$, the axes used to define the Stokes parameters are $\mathbf{e_x}$ and $\mathbf{e_y}$, and

$$C_l^T = \int k^2 dk\, |\Delta_l^T|^2, \quad (6)$$

$$C_l^P = \int k^2 dk\, |\Delta_l^P|^2, \quad (7)$$

$$C_l^{TP} = \frac{(l-2)!}{(l+2)!}\sum_{l'}(2l'+1)\int k^2 dk\, \Delta_{l'}^P \Delta_l^{T*} a_{ll'}, \quad (8)$$

$$C_l^{PP} = \frac{(l-4)!}{(l+4)!}\sum_{l'}(2l'+1)\int k^2 dk\, \Delta_{l'}^P \Delta_l^{P*} \tilde{a}_{ll'}. \quad (9)$$

The constants $a_{ll'}$ and $\tilde{a}_{ll'}$ are given by $a_{ll'} = \int_{-1}^{1} dx\, P_l(x)P_{l'}^2(x)$ and $\tilde{a}_{ll'} = \int_{-1}^{1} dx\, P_l(x)P_{l'}^4(x)$ which have simple closed form expressions. In deriving Eqs. (4) and (5) we further assumed $\theta \ll 1$.

Figure 2 shows $\langle QT\rangle$ for $\phi = 0$. The $\cos 2\phi$ dependence of $\langle QT\rangle$ means that it must vanish at zero angular separation in order to be single valued. The scale of the polarization pattern is limited by the photon mean free path at last scattering, of order the horizon at that time—which subtends an angle of 2° with standard recombination, and 6° for a fully ionized universe.

If the primordial perturbations are Gaussian, so are the temperature and polarization fields. In this case the statistics are completely described by two-point functions. We have constructed realizations of the microwave sky using the small angle approximation, in which spherical harmonics are replaced by plane waves,

$$T(\boldsymbol{\theta}) = \sum_{\mathbf{n}} \tilde{T}(\mathbf{n}) e^{i2\pi\mathbf{n}\cdot\boldsymbol{\theta}/\Theta}, \quad (10)$$

and similarly for Q and U, where Θ is the angular size of the map, and the wave number $\mathbf{n}$ has integer components. Each Fourier mode $\mathbf{n}$ of the temperature anisotropy field T is allocated a random Gaussian-distributed, complex variable $\zeta_1(\mathbf{n})$ with zero mean and unit variance $\langle\zeta_1^*\zeta_1\rangle = 1$, according to $\tilde{T}(\mathbf{n}) = (C_l^T)^{1/2}\zeta_1(\mathbf{n})$, where $l \simeq (2\pi/n\Theta)$. A second independent random variable ζ_2 is used to define the Q Fourier modes:

$$\tilde{Q}(\mathbf{n}) = [\tilde{Q}_C(\mathbf{n})\zeta_1(\mathbf{n}) + \tilde{Q}_U(\mathbf{n})\zeta_2(\mathbf{n})]\cos 2\phi_n, \quad (11)$$

where $\tilde{Q}_C(\mathbf{n})$ and $\tilde{Q}_U(\mathbf{n})$ are chosen to reproduce the $\langle QT\rangle$ and $\langle QQ\rangle$ correlation functions and ϕ_n is the usual polar angle of the vector $\mathbf{n}$. The U modes are allocated in a similar way.

The polarization field is therefore a sum of two components, which are, respectively, correlated, $Q_C(\boldsymbol{\theta})$, and uncorrelated, $Q_U(\boldsymbol{\theta})$, with the temperature anisotropy. Figure 3 shows the correlated component overlaid on the temperature field. The length of each vector is proportional to $[Q_C^2(\boldsymbol{\theta}) + U_C^2(\boldsymbol{\theta})]^{\frac{1}{2}}$ and the orientation is given by $2\phi = \tan^{-1}(U_C/Q_C)$. There are clear correspondences between the temperature and the correlated polarization. The most obvious features are seen around hot and cold spots in an otherwise uniform background, with radial and tangential polarization patterns, respectively. *Note that the figure only shows the correlated component of the polarization—the effect of including the larger uncorrelated component is to mask almost entirely all obvious correspondences with the temperature map.*

The correlated part of the polarization is a small part of the total signal. Figure 4 shows the power spectra of the temperature-correlated polarization $\langle Q_C Q_C \rangle$ and the total polarization $\langle QQ \rangle$. The variance of the total polarization σ_Q^2, corresponding to the area beneath the curve, is approximately 7 times that of its correlated component $\sigma_{Q_C}^2$. (The ratio for the constantly ionized universe is similar.) From a measured map of the temperature anisotropy, it is straightforward to construct a map of the correlated part of the polarization, as we have done in Fig. 3. Because the uncorrelated part of the polarization is large, the map of the correlated part is a useful predictor of the total polarization in only a statistical sense. A one-to-one correspondence between features in the temperature-correlated map and those in the total polarization is not expected. However, one is much more likely to find a peak in the total polarization at a peak in the correlated map than at a random point in the sky.

This statement can be quantified. The probability of finding an $n\sigma_Q$ peak in the total polarization if one is at an $m\sigma_{Q_C}$ peak in the correlated polarization is

$$p = \frac{1}{[2\pi(\sigma_Q^2 - \sigma_{Q_C}^2)]^{\frac{1}{2}}} \exp\left[\frac{-(n\sigma_Q - m\sigma_{Q_C})^2}{2(\sigma_Q^2 - \sigma_{Q_C}^2)}\right], \tag{12}$$

while the probability of finding an $n\sigma$ peak by looking at a random point in the sky is $e^{-n^2/2}/(2\pi\sigma_Q^2)^{\frac{1}{2}}$. Thus, for example, the odds of finding a $1\sigma_Q$ peak in the total polarization at a $3\sigma_{Q_C}$ peak in the correlated polarization are 3 times greater than at a random point. If degree scale temperature anisotropy maps become available, it may be useful to construct the map of correlated polarization (in a given theoretical scenario) and use it as a guide to the "best" points at which to observe the polarization.

Although one expects the correlated polarization to be small, one can attempt to measure $\langle QT \rangle$ directly. This could prove easier than measuring $\langle Q^2 \rangle$ because it is less susceptible to noise in the polarization measurement. Consider a detection obtained from N measurements of the polarization $Q_i \pm \sigma_D$, where σ_D is the detector noise. If the measurements are sufficiently isolated from each other to be uncorrelated, then the measured variance will be

$$Q^2|_{\text{meas}} = \sigma_Q^2 \pm \sqrt{\frac{2}{N}}[\sigma_Q^2 + \sigma_D^2], \tag{13}$$

where σ_Q^2 is the true polarization variance. Whereas, the measured temperature-polarization correlation will be

$$QT(\theta,\phi)|_{\text{meas}} = \langle QT(\theta,\phi)\rangle \pm \sqrt{\frac{\sigma_T^2}{N}}[\sigma_Q^2 + \sigma_D^2]^{\frac{1}{2}}, \tag{14}$$

where σ_T^2 is the variance of the temperature anisotropy. (We have assumed that the noise in the temperature anisotropy is negligible.) In the limit of large detector

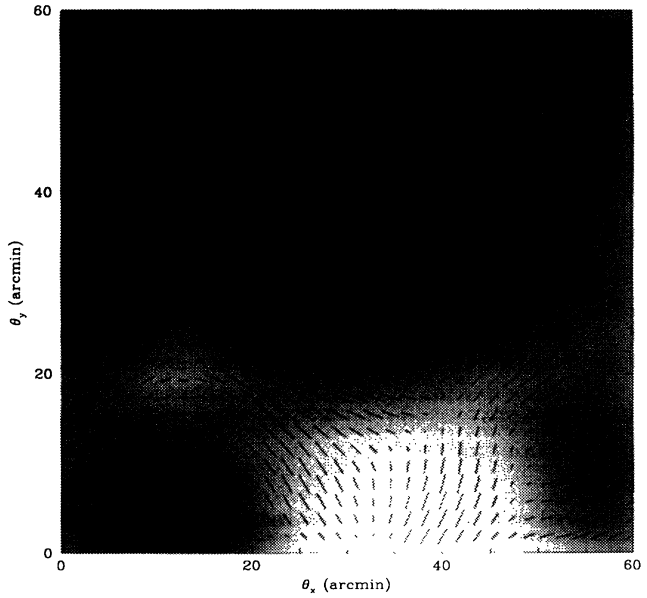

FIG. 3. $1° \times 1°$ temperature map (smoothed with a Gaussian beam with FWHM of $10'$) with the correlated component of the polarization overlaid.

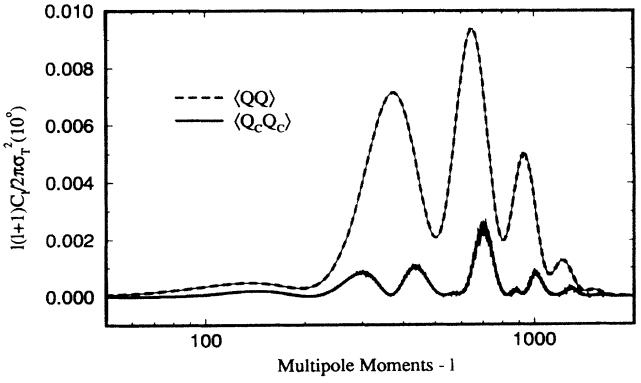

FIG. 4. The power spectra (smoothed on a scale of $10'$) of the total (dashed line) and temperature-correlated (solid line) polarization in a universe with a standard thermal history normalized to the COBE satellite measurement of the temperature variance with $10°$ smoothing.

noise, the error in measuring Q^2 grows as σ_D^2 while the error in QT grows as σ_D, so that it becomes more advantageous to search for QT correlations.

If one has a full sky temperature map but only a sparsely sampled polarization map, the noise in $\langle QT\rangle$ can be reduced by including all of the temperature information. For example, we can calculate the expected correlation between the polarization at a given point and the temperature in a ring of radius θ about that point. Since $\langle QT\rangle$ is proportional to $\cos 2\phi$, if we define $\bar{T}(\theta) = \frac{1}{2\pi} \times \int d\phi T(\theta,\phi)\cos 2\phi$, then $\langle Q\bar{T}(\theta)\rangle = \langle QT(\theta,\phi = 0°)\rangle/2$. The error in measuring $\langle Q\bar{T}(\theta)\rangle$ is reduced significantly because $\bar{T}(\theta)$ is an average over a number of uncorrelated patches. Thus, the variance in $\bar{T}(\theta)$, $\langle \bar{T}^2(\theta)\rangle = \frac{1}{4\pi}\int d\phi \cos 2\phi\, C_T(\theta\sqrt{2-2\cos\phi})$, is much smaller than the variance in the temperature anisotropy itself. For a ring of radius θ, $\bar{T}$ is a weighted average of $I \sim \pi\theta/\theta_c$ independent patches (where θ_c is the temperature correlation angle) and its variance is $\langle \bar{T}^2(\theta)\rangle \sim \sigma_T^2/2I$. Assuming the rings about the polarization measurements do not have substantial overlap, this increases the signal to noise of $\langle Q\bar{T}(\theta)\rangle$ by a factor of $\sqrt{I/2}$ over that of $\langle QT(\theta)\rangle$.

Alternatively, one can test the correlated polarization map (constructed as described above) by measuring the weighted average $\langle Q_C^{\text{theory}} Q\rangle$. For N uncorrelated measurements of the polarization,

$$Q_C^{\text{theory}} Q|_{\text{meas}} = \sigma_{Q_C}^2 \pm \sqrt{\frac{\sigma_{Q_C}^2}{N}}[\sigma_Q^2 + \sigma_D^2]^{\frac{1}{2}}. \qquad (15)$$

Comparing the signal to noise of $\langle Q^2\rangle$ and $\langle Q_C^{\text{theory}} Q\rangle$, and using $\sigma_{Q_C}^2 \sim \sigma_Q^2/7$, one finds that if the noise is greater than the polarization signal, $\sigma_D \gtrsim 1.5\sigma_Q$, then it becomes easier to measure $\langle Q_C Q\rangle$ than $\langle Q^2\rangle$.

Consider a hypothetical experiment which measures the polarization with a 0.5° FWHM beam of 1000 well separated patches on the sky. The expected polarization for a standard recombination model is $\sigma_Q \simeq 1.4\ \mu$K, while the correlated polarization signal is about one-third of this. If the noise level can be reduced to 3 μK per pixel, the signal to noise of the polarization variance $\langle Q^2\rangle$ and that of $\langle Q_C^{\text{theory}} Q\rangle$ are both about 5 to 1, while the signal to noise of the $\langle Q\bar{T}(\theta)\rangle$ is approximately 3 to 1 on an angular scale $\theta \simeq 1.3°$. For a fully sampled polarization map the signal to noise would improve. For the no-recombination case, the expected noise levels are comparable to these because even though the variance of the polarization on 0.5° is larger ($\simeq 3\ \mu$K), the correlation angle is also larger and fewer independent measurements can be made from the same sky coverage. These numbers ignore any other noncosmological sources of polarization, but on such large angular scales one can hope that astrophysical sources, e.g., radio galaxies, hot gas in clusters, do not contribute significantly.

Given a fixed integration time, the optimal observation strategies for measuring $\langle QT\rangle$ and $\langle QQ\rangle$ differ significantly. If the noise σ_D is statistical, i.e., inversely proportional to the square root of the time spent in making the observation, then the best strategy for measuring the polarization variance is to spend enough time at each observation such that σ_D is comparable to σ_Q before moving on. The optimal strategy for measuring $\langle Q\bar{T}(\theta)\rangle$, however, is to maximize the number of observations, independent of the noise level, i.e., to map out the polarization over the whole sky. Such a strategy might most easily be realized in conjunction with a full sky anisotropy mapping experiment such as those presently being planned.

To conclude, the temperature-polarization correlation provides another observable quantity which may be used to probe the physics of the density perturbations on the surface of last scattering. Although the magnitude of the effect is small, we have shown that a reasonable signal to noise ratio is within reach of projected experiments. We intend to extend the calculations reported here to other cosmological parameters and structure formation scenarios, such as baryon isocurvature and defect models.

We thank K. Ganga, P. J. E. Peebles, and D. Wilkinson for useful conversations. R. C. thanks R. Davis and P. Steinhardt for collaborating in the initial development of the Boltzmann code. The work of D. C. was supported by EPSRC (UK), while that of R. C. and N. T. was partially supported by NSF Contract No. PHY90-21984, and the David and Lucile Packard Foundation.

[1] G. F. Smoot *et al.,* Astrophys. J. **396**, L1 (1992).
[2] J. R. Bond *et al.,* Phys. Rev. Lett. **72**, 13 (1994).
[3] P. J. E. Peebles, Astrophys. J. **315**, L73 (1987); Princeton University Report, 1994 (to be published).
[4] D. Coulson *et al.,* Nature (London) **368**, 27 (1994).
[5] M. J. Rees, Astrophys. J. **153**, L1 (1968).
[6] C. J. Hogan, N. Kaiser, and M. J. Rees, Philos. Trans. R. Soc. London A, **307**, 97 (1982).
[7] J. R. Bond and G. Efstathiou, Mon. Not. R. Astron. Soc. **226**, 655 (1987).
[8] R. Crittenden, R. Davis, and P. Steinhardt, Astrophys. J. **417**, L13 (1993).
[9] P. M. Lubin, P. Melese, and G. F. Smoot, Astrophys. J. **273**, L51 (1983).
[10] R. B. Partridge, J. Nowakowski, and H. M. Martin, Nature (London) **331**, 146 (1988).
[11] E. J. Wollack *et al.,* Astrophys. J. **419**, L49 (1993).
[12] S. Chandrasekhar, *Radiative Transfer* (Dover, New York, 1960), pp. 1–53.
[13] A. G. Polnarev, Sov. Astr. **29**, 607 (1985).
[14] J. R. Bond and G. Efstathiou, Astrophys. J. **285**, L45 (1984).
[15] N. Kaiser, Mon. Not. R. Astron. Soc. **202**, 1169 (1983).

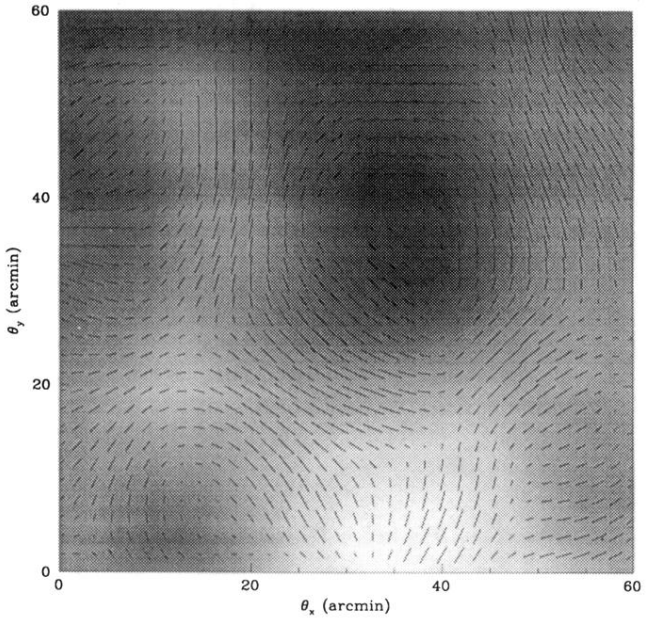

FIG. 3. $1° \times 1°$ temperature map (smoothed with a Gaussian beam with FWHM of $10'$) with the correlated component of the polarization overlaid.